Evaluation of Orbiter Performance and Nose Heating at Mach 3.8

By: Nicholas Zhu

February 26, 2020

1 Introduction

1.1 3-D orbiter shape

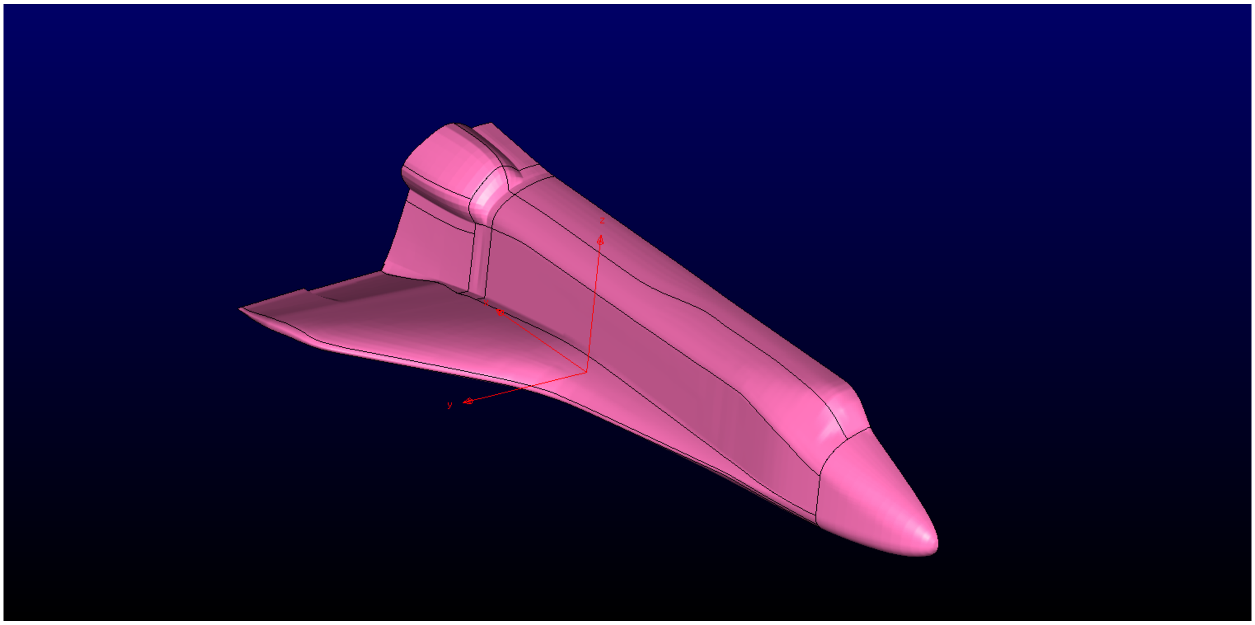

Figure 1: 3-D orbiter

1.2 Data from Published Texts

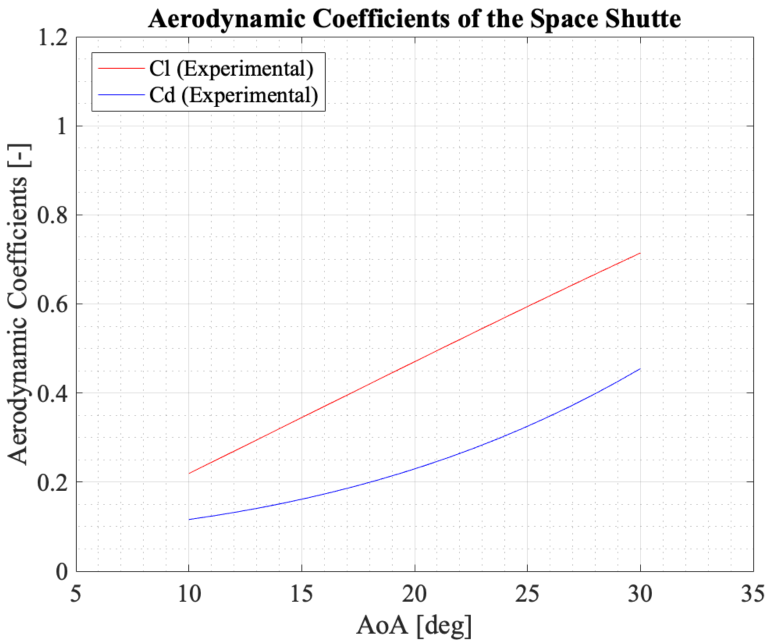

Figure 2: Experimental models and predictions of C_L & C_D for M = 3.8

The equations used to plot the data in figure 2 were from [2].

Table 1: Freestream conditions and expected stagnation conditions at wing/nose LE

Mach number	3.8
Post-normal shock mach number	0.4407
Absolute pressure p	1090.16 Pa
Temperature T	227.13 K
Density ρ	0.0167 $\text{kg} \cdot \text{m}^{-3}$
$^{p_2}/_{p_1}$ at M=3.8	16.68
$^{T_2}/_{T_1}$ at M=3.8	3.743
Isentropic $^{p_o}/_{p}$ at M=0.44	1.142
Isentropic $^{T_o}/_{T}$ at M=0.44	1.035
Stagnation pressure	20765.98 Pa $(p \cdot {}^{p_2}/_{p_1} \cdot {}^{p_o}/_{p})$
Stagnation temperature	883.303 K $(T \cdot {}^{T_2}/_{T_1} \cdot {}^{T_o}/_{T})$

p, T, ρ: at 100,000 ft from 1976 Digital Dutch Standard Atmospheric Calculator (URL: https://www.digitaldutch.com/atmoscalc/)

Isentropic relations and pressure/temp discontinuity across shock: From appendix A of Modern Compressible Flow by J.D. Anderson [1].

2 Methodology

2.1 Shots of the Orbiter grid

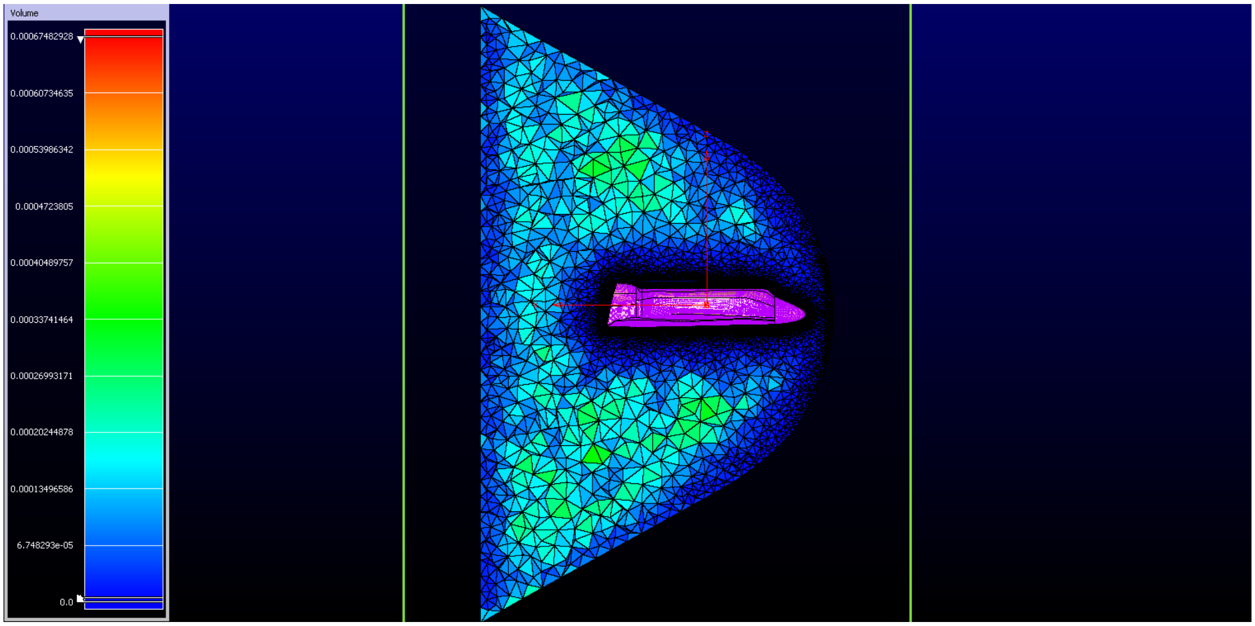

Figure 3: Entire grid of the orbiter

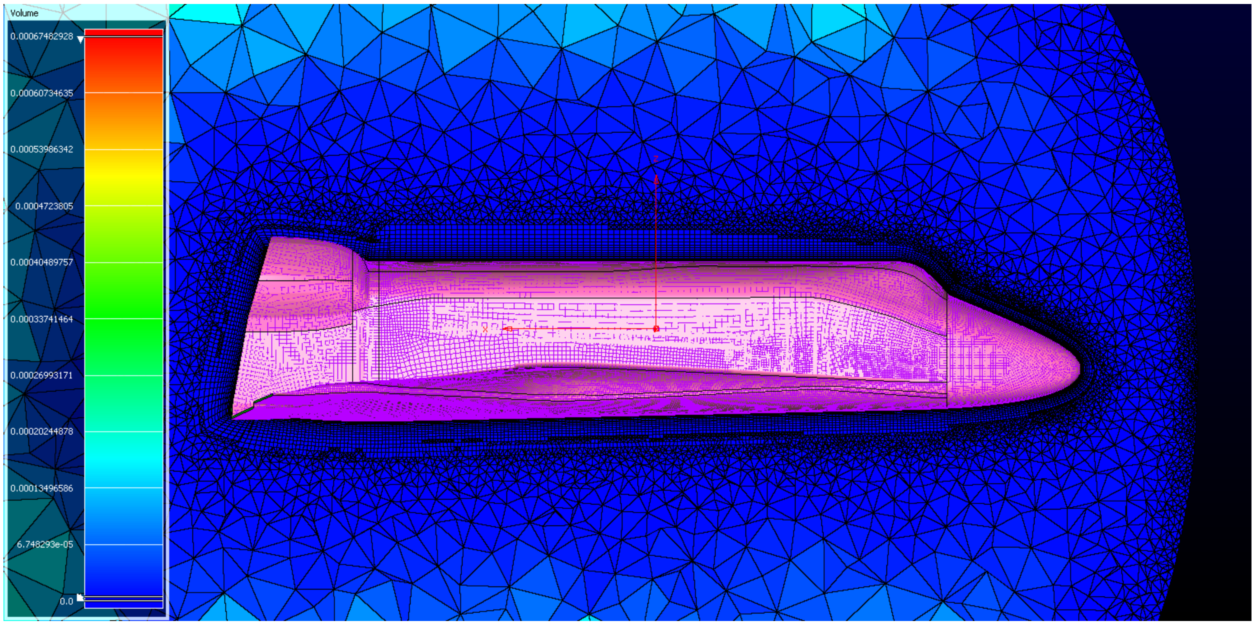

Figure 4: Surface grid of the orbiter

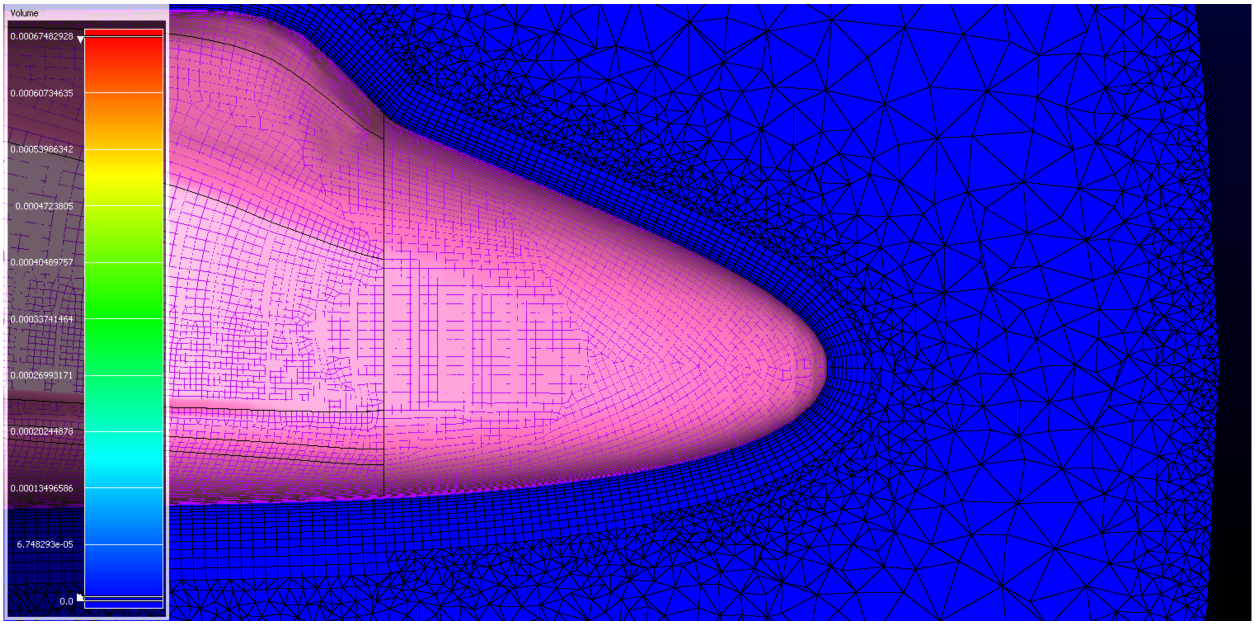

Figure 5: Nose of the orbiter

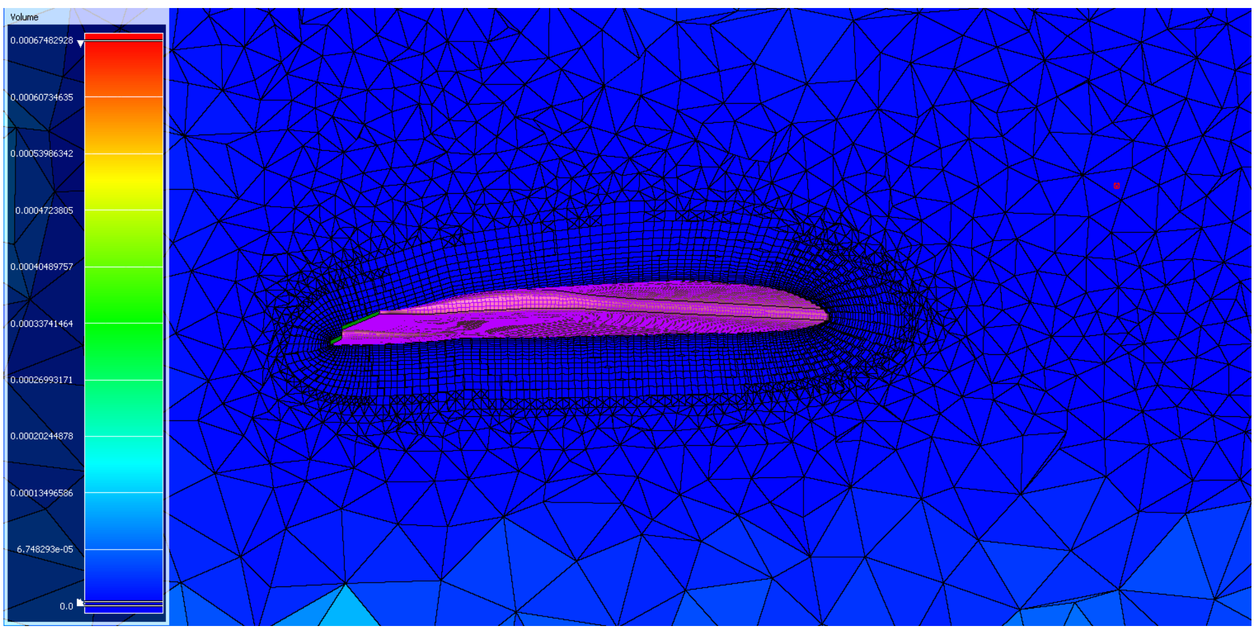

Figure 6: Midspan of the wing of the orbiter

2.2 Fluent setup

Table 2: General grid information

Cell count	1,375,480 Cells
Min/max included angles	**max**: 179.844 deg **min**: 0.06222 deg
Normal-to-wall spacing	$\mathbf{\Delta s}$ = 0.001 m
Boundary conditions	**Inlet/hemispherical shell**: pressure far-field **Outlet/back of hemispherical shell**: pressure outlet **Orbiter surface (including backside)**: wall **Plane of Symmetry**: symmetry
Reference values	**Area**: 257.47 [m^2] **Density**: 1.672e-02 [kg$\cdot$ m^{-3}] **Enthalpy**: 8.907e+05 [J$\cdot$ kg^{-3}] **Length**: 38.424 [m] **Gauage pressure**: 0 [Pa] **Temperature**: 227.13 [K] **Velocity**: 1147.86 [m$\cdot$ s^{-1}] **Viscosity**: 1.789e-05 [kg$\cdot$ $m^{-1}s^{-1}$] **Ratio of specific heat**: 1.4
Submodels	**Density**: ideal-gas **Specific heat**: piece-wise polynomial **Thermal conductivity**: kinetic-theory **Viscosity**: sutherland
Numerical Scheme	Implicit AUSM
Spatial Discretization	**Gradient**: least-squares cell based **Flow**: first order upwind

3 Results

3.1 Proof of convergence history

Pleas see Appendix

3.2 Table of final lift and drag coefficients and related forces

Case [°]	C_L [-]	C_D [-]	Lift [N]	Drag [N]
10	0.143	0.075	405,550	212,700
20	0.341	0.174	967,090	493,470
30	0.545	0.371	1,545,600	1,052,200

3.3 Plot of lift and drag and L/D vs. AOA with peak L/D identified

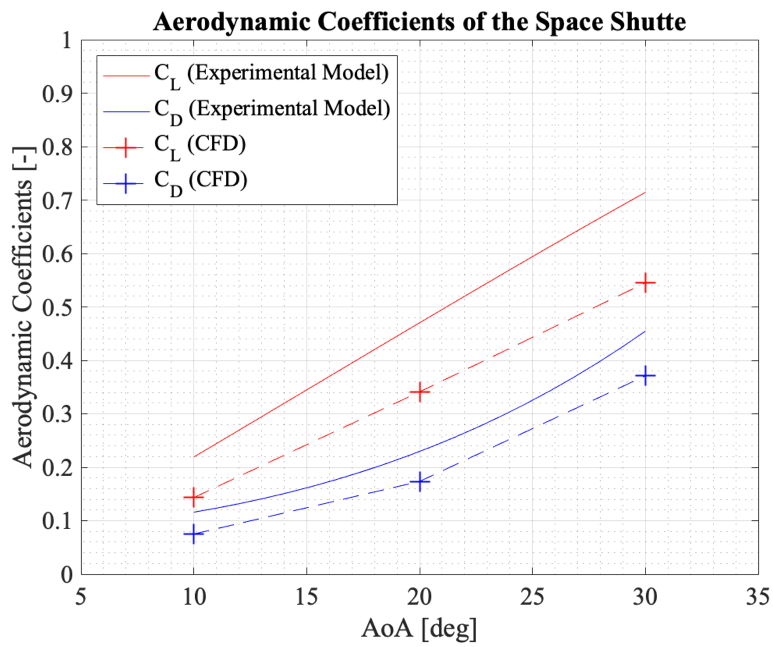

Figure 7: Comparison of the C_L and C_D results from the experimental model and the CFD cases ran

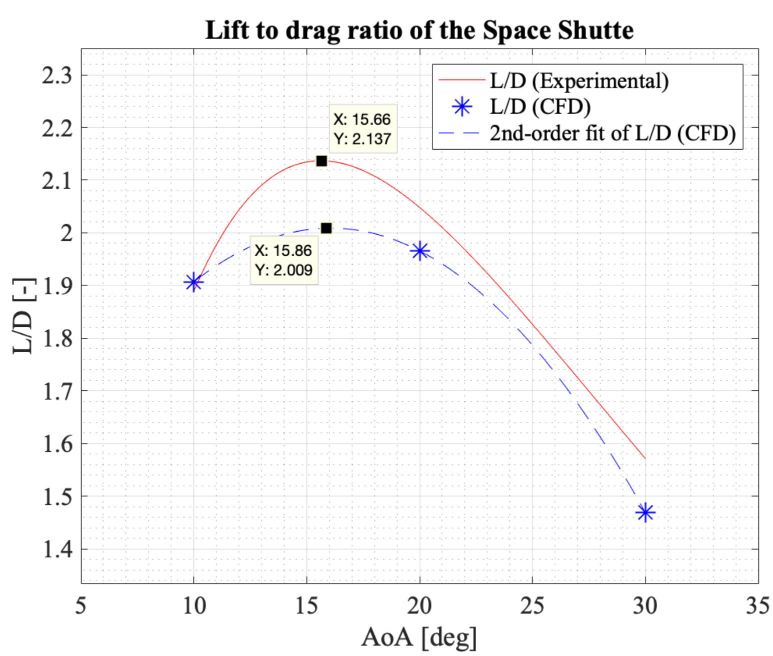

Figure 8: Comparison of the lift-to-drag ratios from the experimental model and the CFD cases ran

3.4 Pressure and temperature contours with streamlines

3.4.1 AoA = 10°

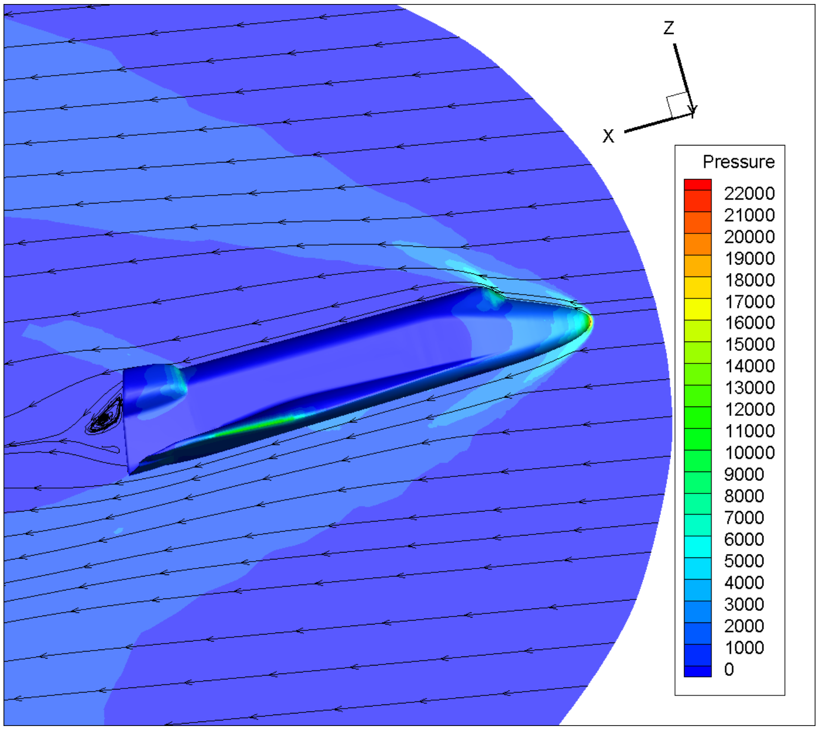

(a) Pressure contour at the symmetry plane of the orbiter at 10 degs AoA

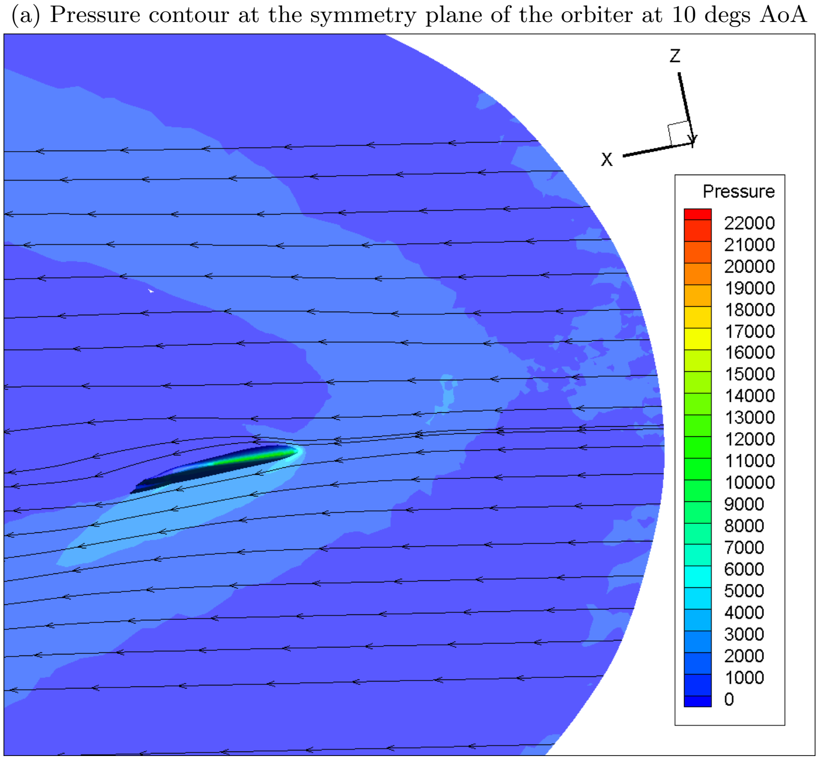

(b) Pressure contour at the midspan of the wing of the orbiter at 10 degs AoA

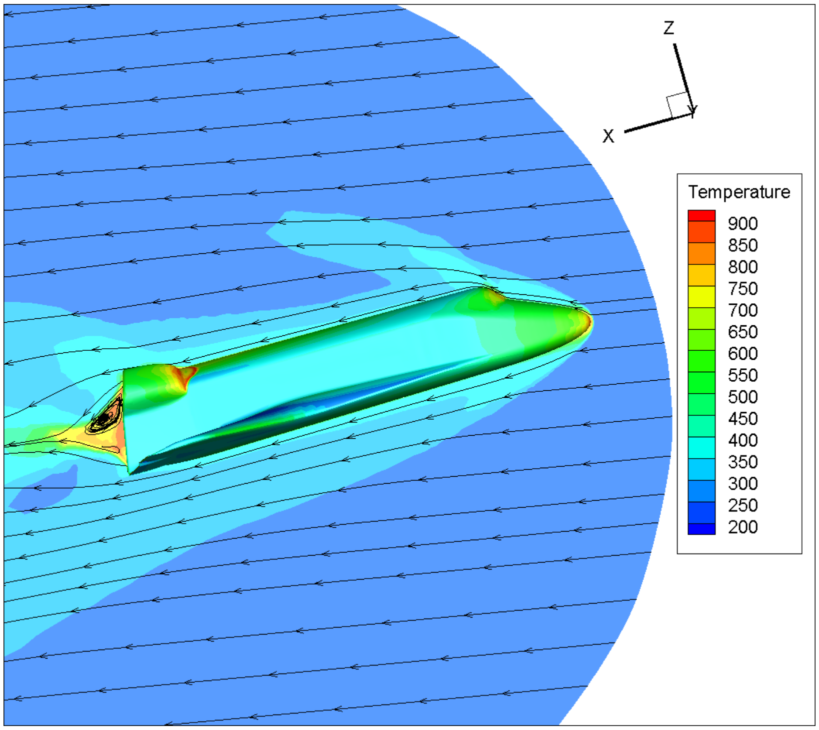

(a) Temperature contour at the symmetry plane of the orbiter at 10 degs AoA

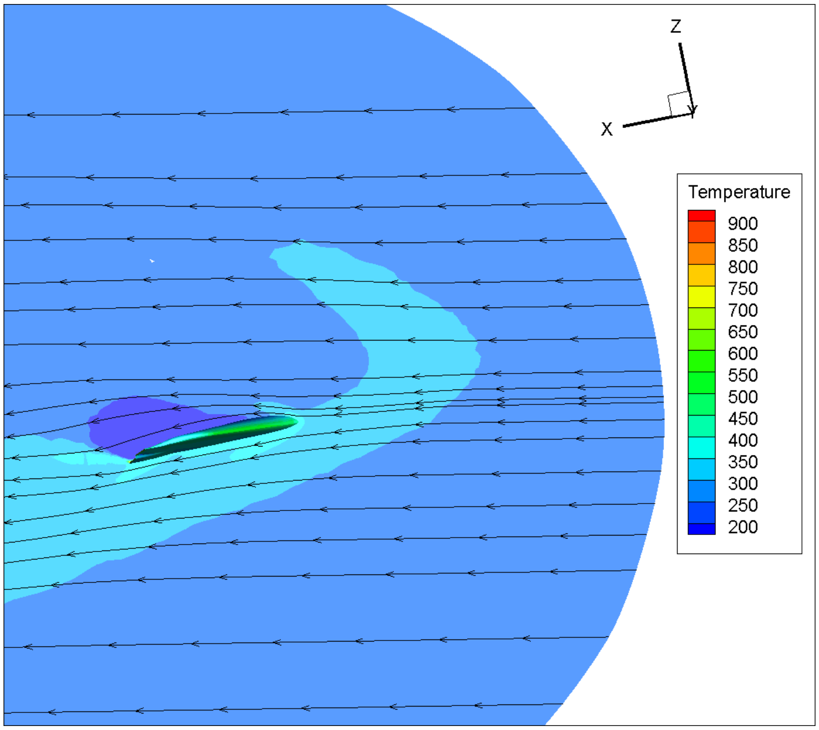

(b) Temperature contour at the midspan of the wing of the orbiter at 10 degs AoA

3.4.2 AoA = 20°

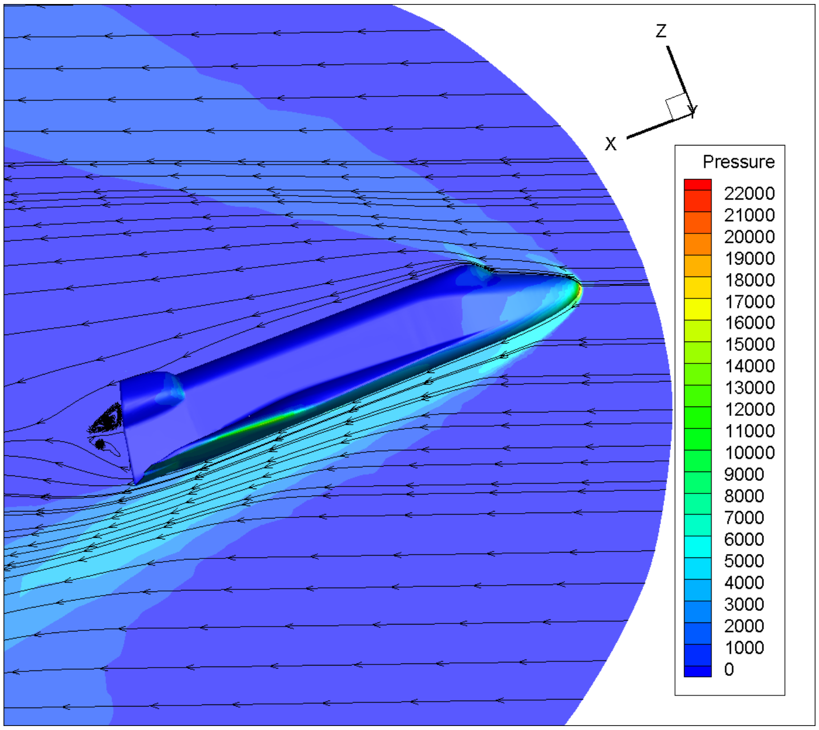

(a) Pressure contour at the symmetry plane of the orbiter at 20 degs AoA

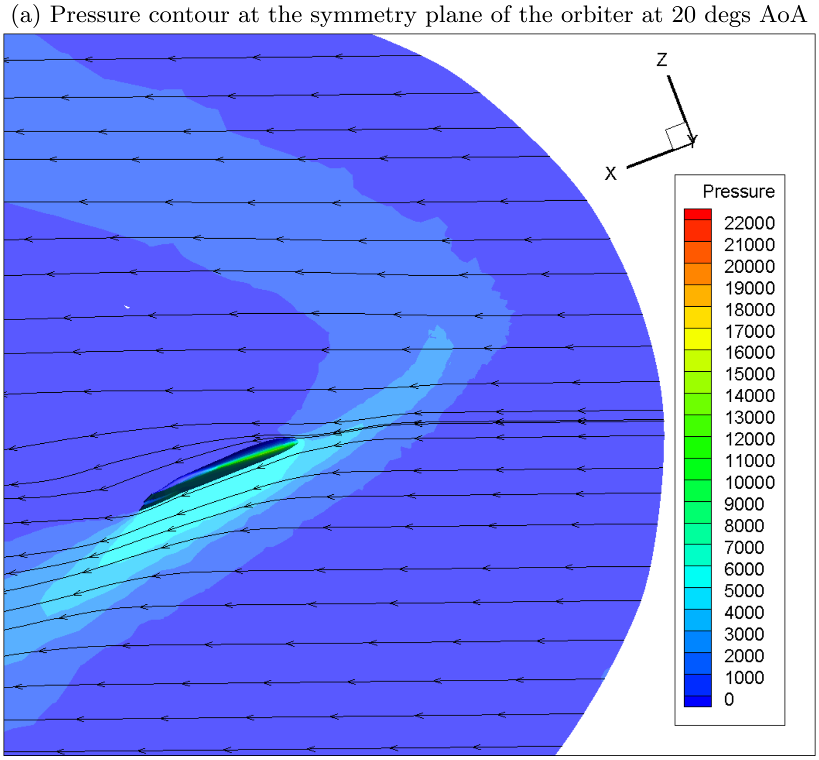

(b) Pressure contour at the midspan of the wing of the orbiter at 20 degs AoA

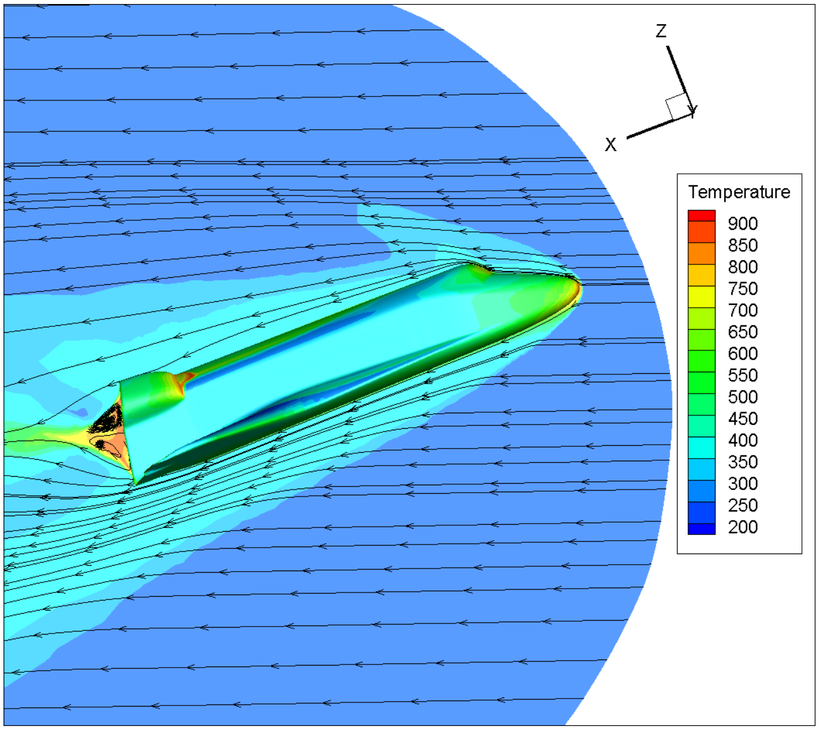

(a) Temperature contour at the symmetry plane of the orbiter at 20 degs AoA

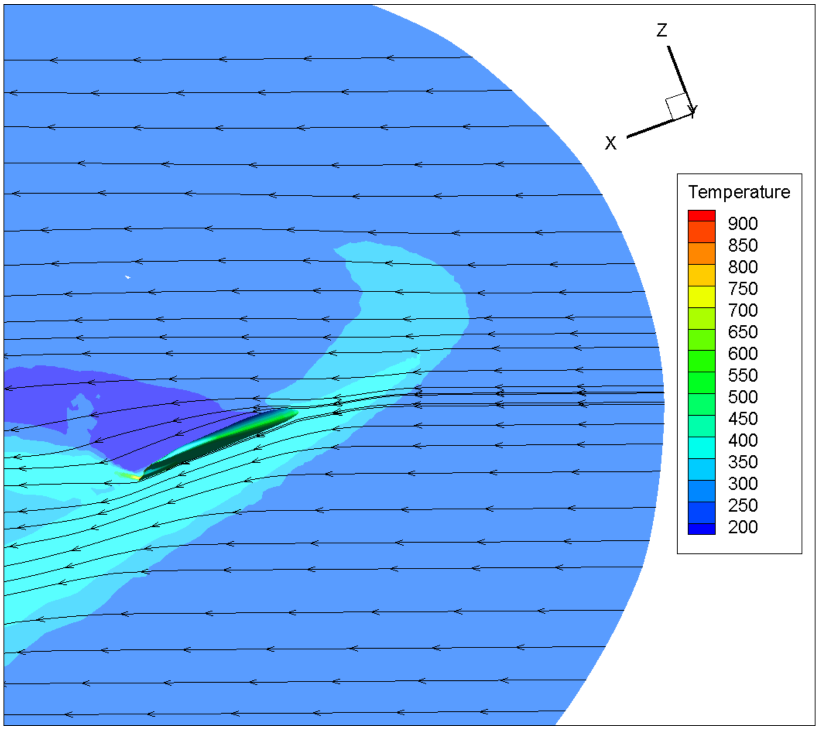

(b) Temperature contour at the midspan of the wing of the orbiter at 20 degs AoA

3.4.3 AoA $= 30^{\circ}$

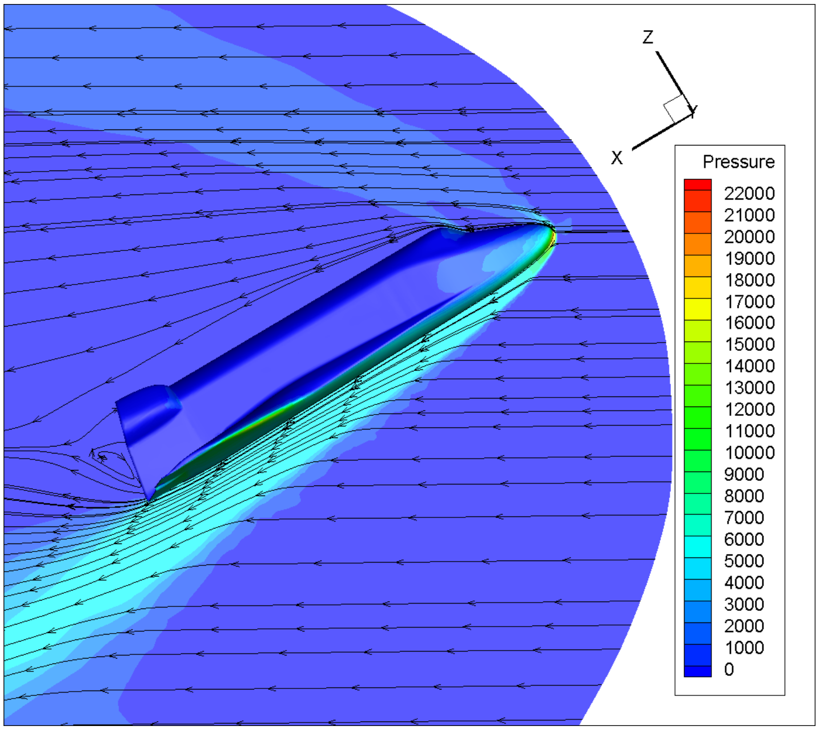

(a) Pressure contour at the symmetry plane of the orbiter at 30 degs AoA

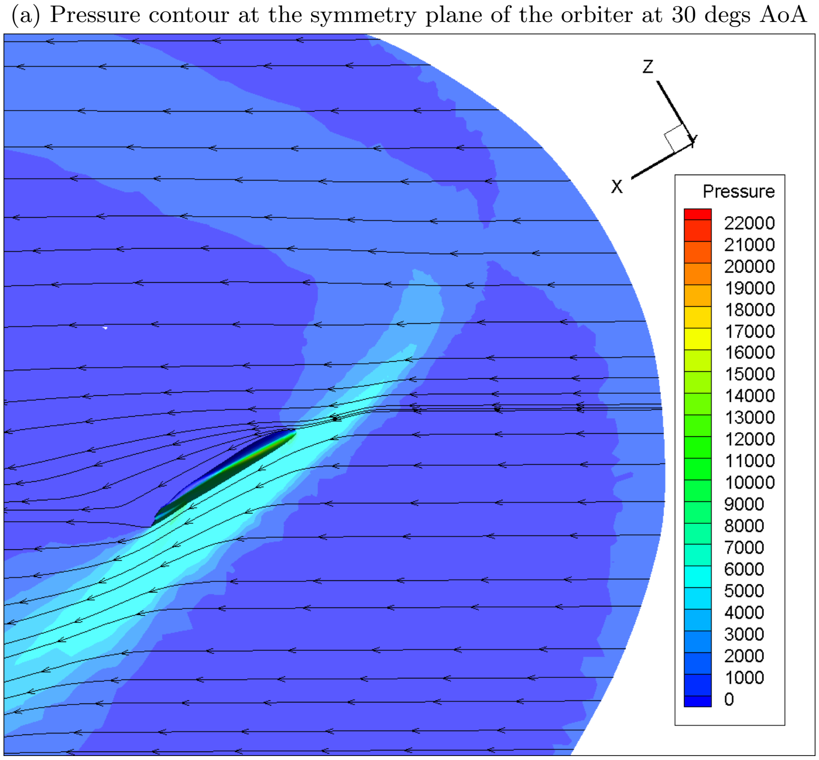

(b) Pressure contour at the midspan of the wing of the orbiter at 30 degs AoA

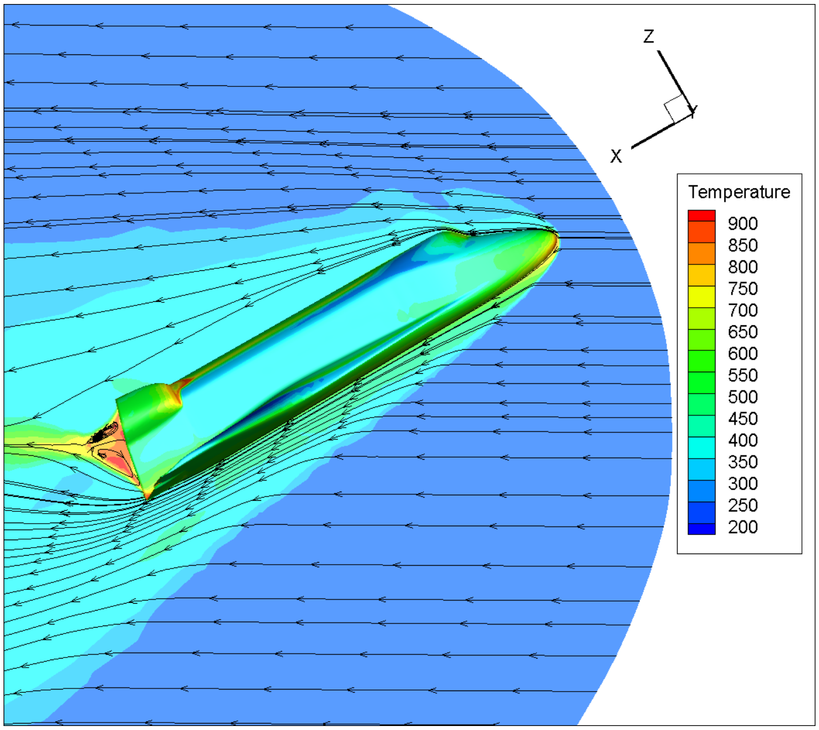

(a) Temperature contour at the symmetry plane of the orbiter at 30 degs AoA

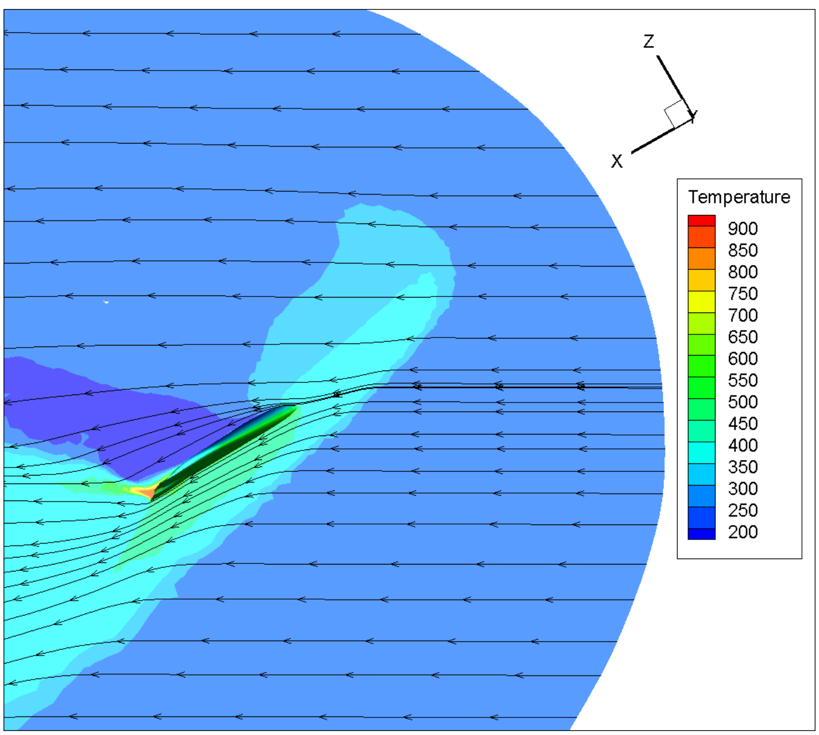

(b) Temperature contour at the midspan of the wing of the orbiter at 30 degs AoA

3.5 Results of grid adaptation

3.5.1 Side by side of contour plots

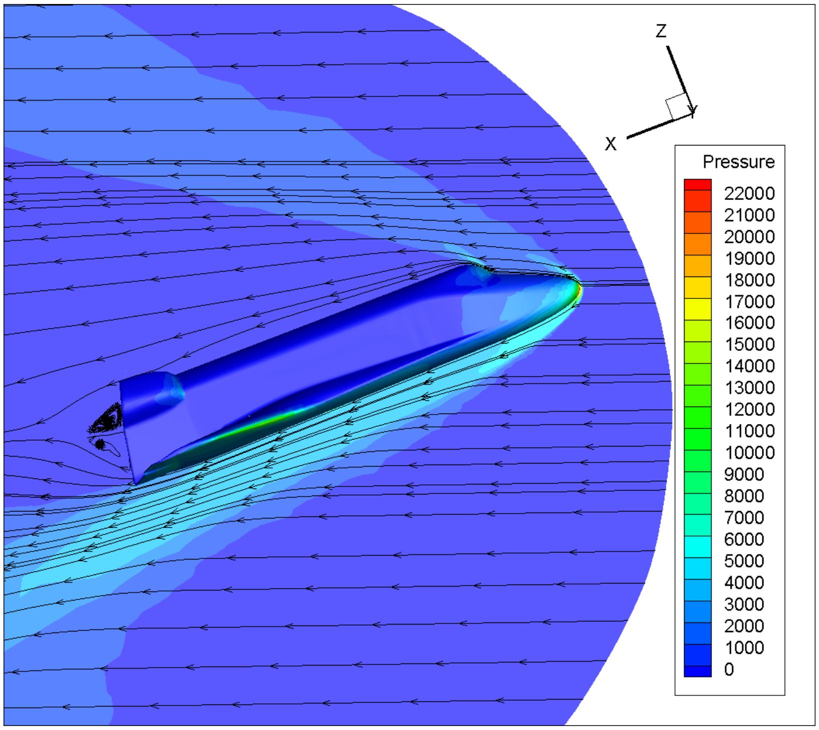

(a) Pressure contour at the symmetry plane of the orbiter at 20 degs AoA

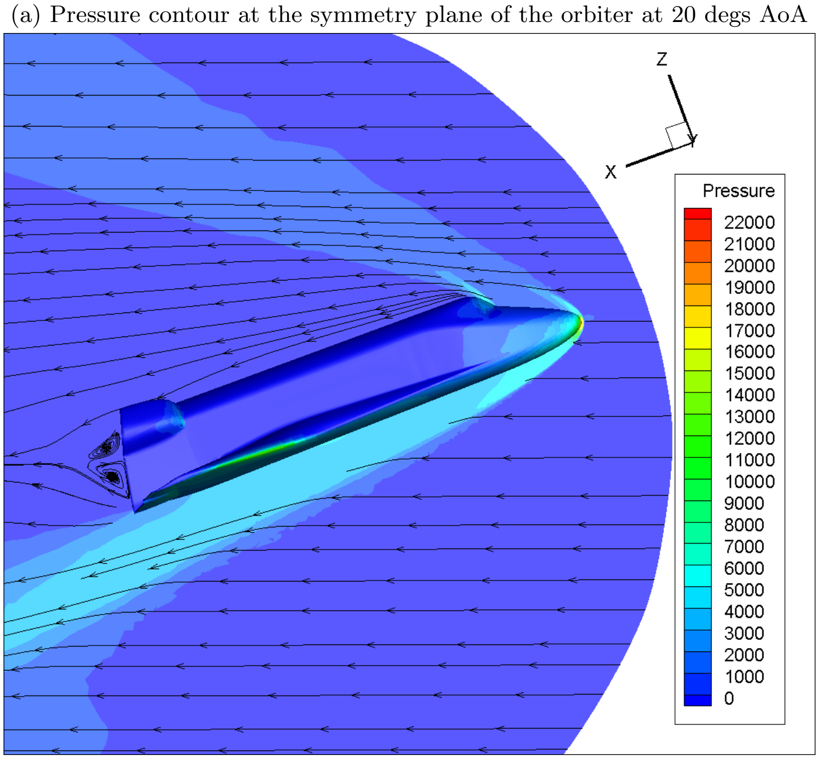

(b) Pressure contour at the symmetry plane of the orbiter at 20 degs AoA using adapted grid

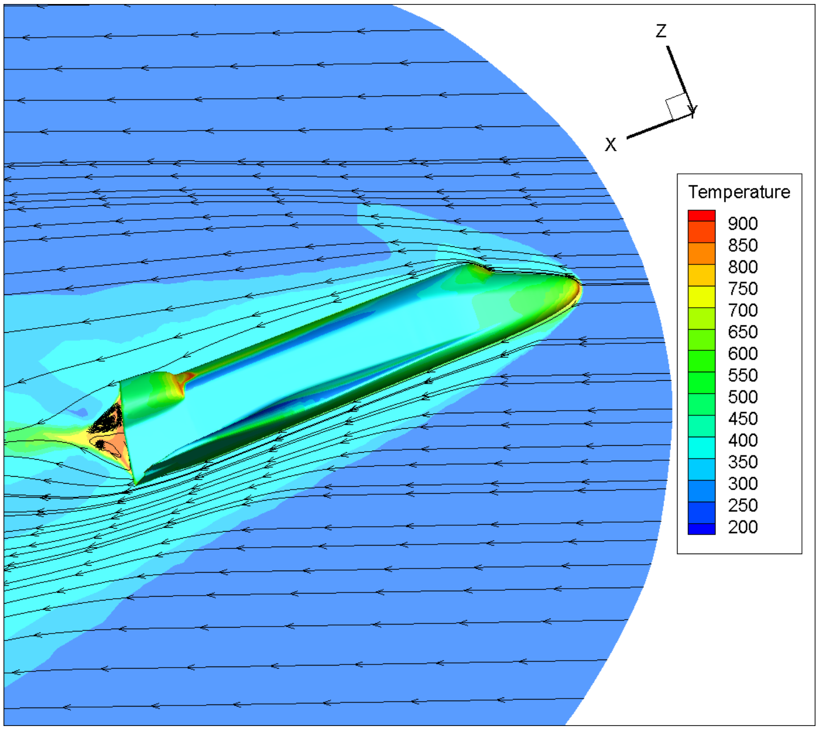

(a) Temperature contour at the symmetry plane of the orbiter at 20 degs AoA

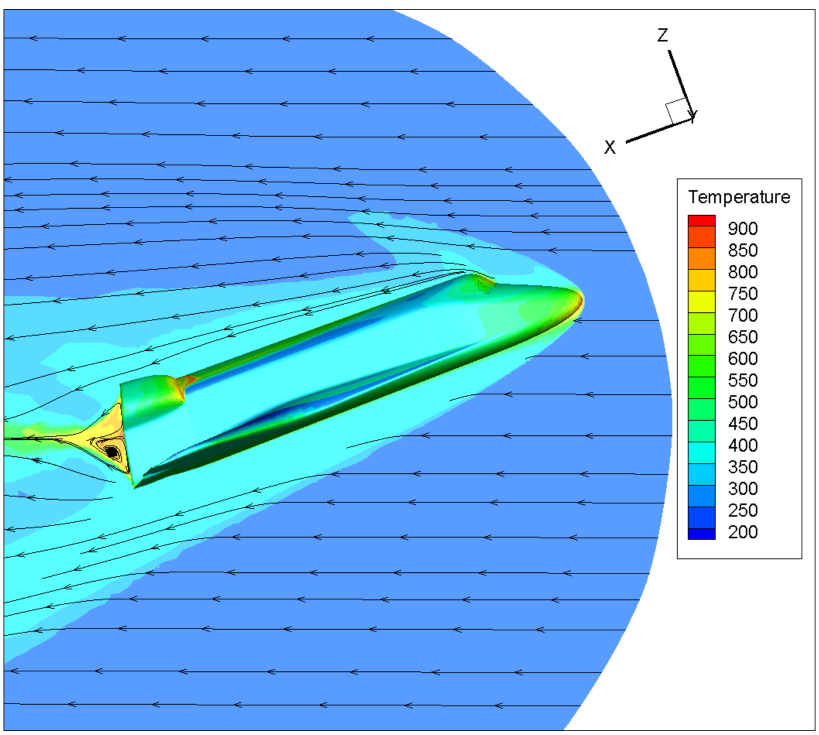

(b) Temperature contour at the midspan of the wing of the orbiter at 20 degs AoA using adapted grid

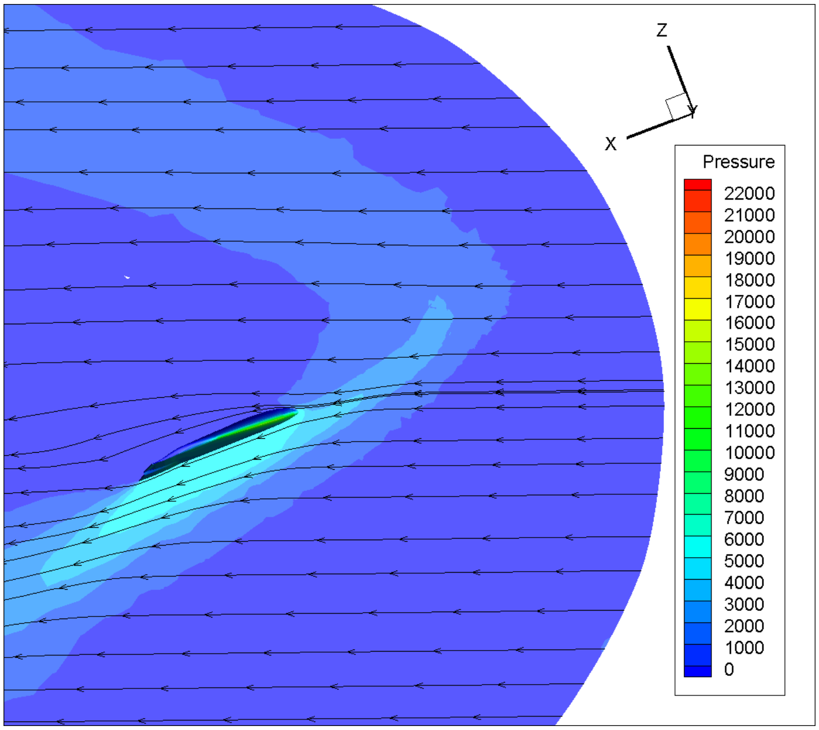

(a) Pressure contour at the midspan of the wing of the orbiter at 20 degs AoA

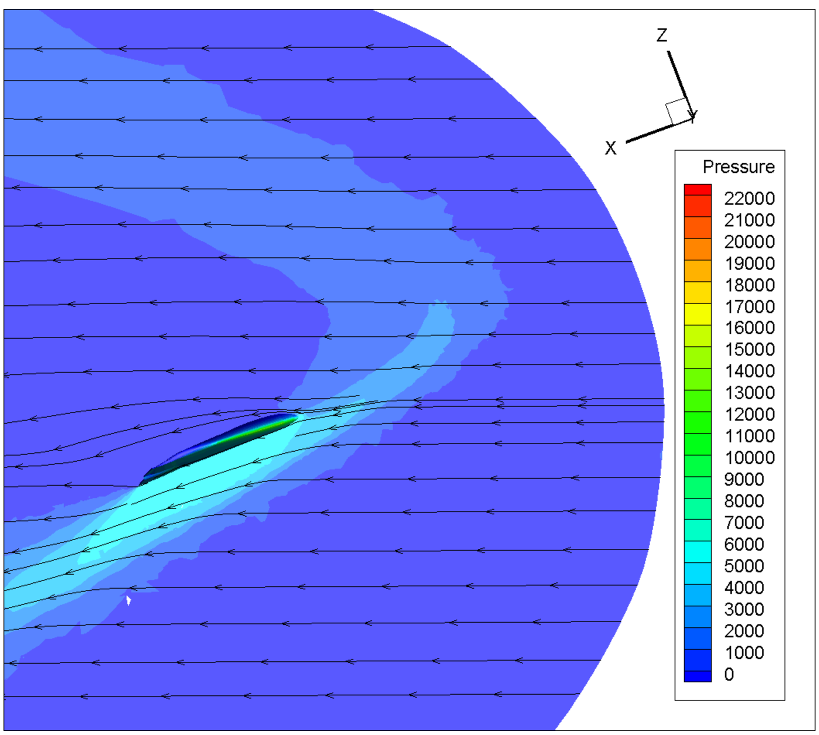

(b) Pressure contour at the midspan of the wing of the orbiter at 20 degs AoA using adapted grid

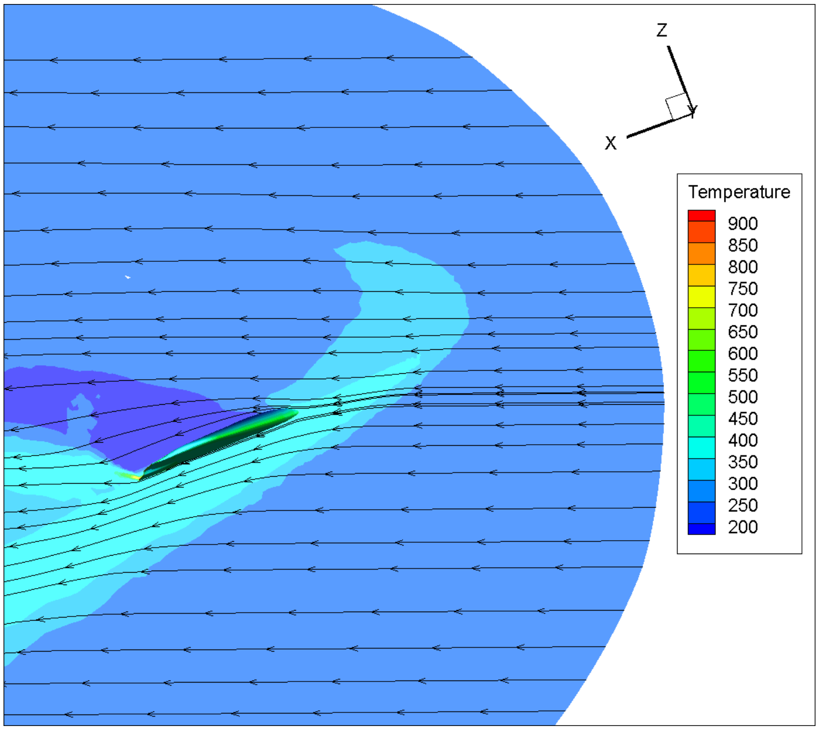

(a) Temperature contour at the midspan of the wing of the orbiter at 20 degs AoA

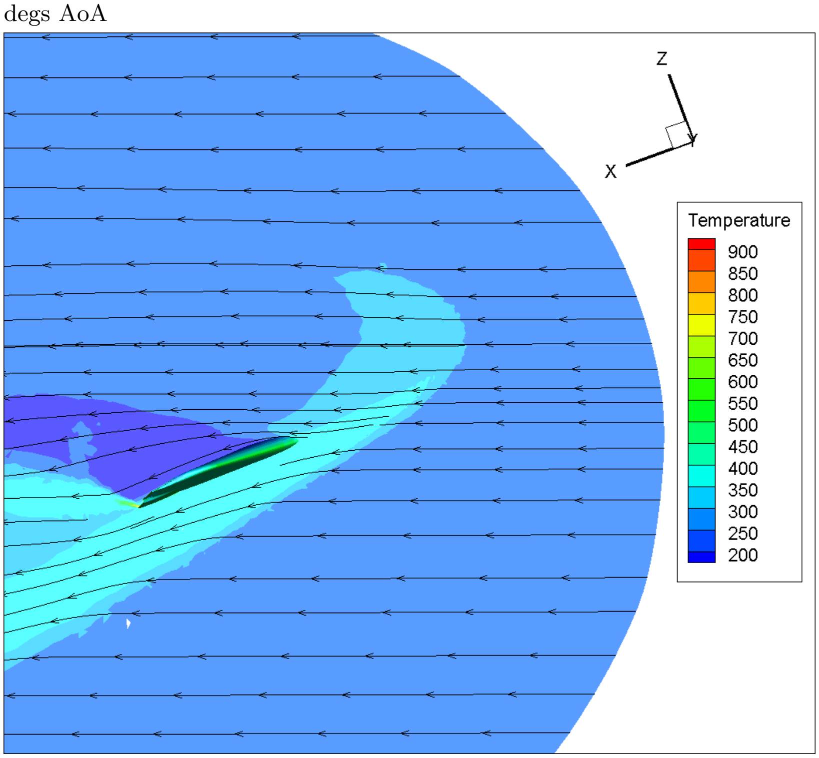

(b) Temperature contour at the midspan of the wing of the orbiter at 20 degs AoA using adapted grid

3.5.2 Side by side of mesh

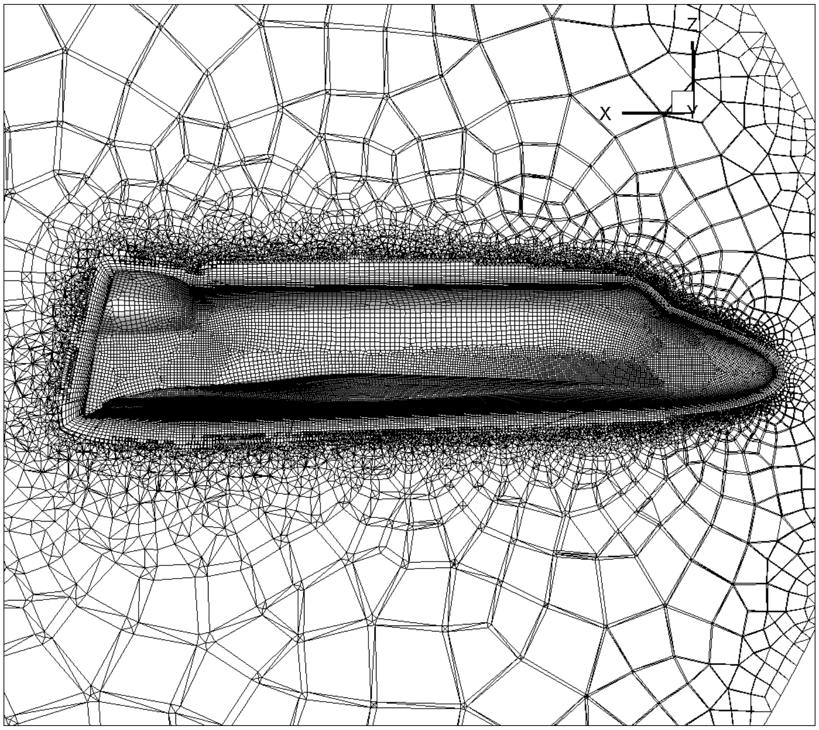

(a) Grid at the symmetry plane of the orbiter at 20 degs AoA

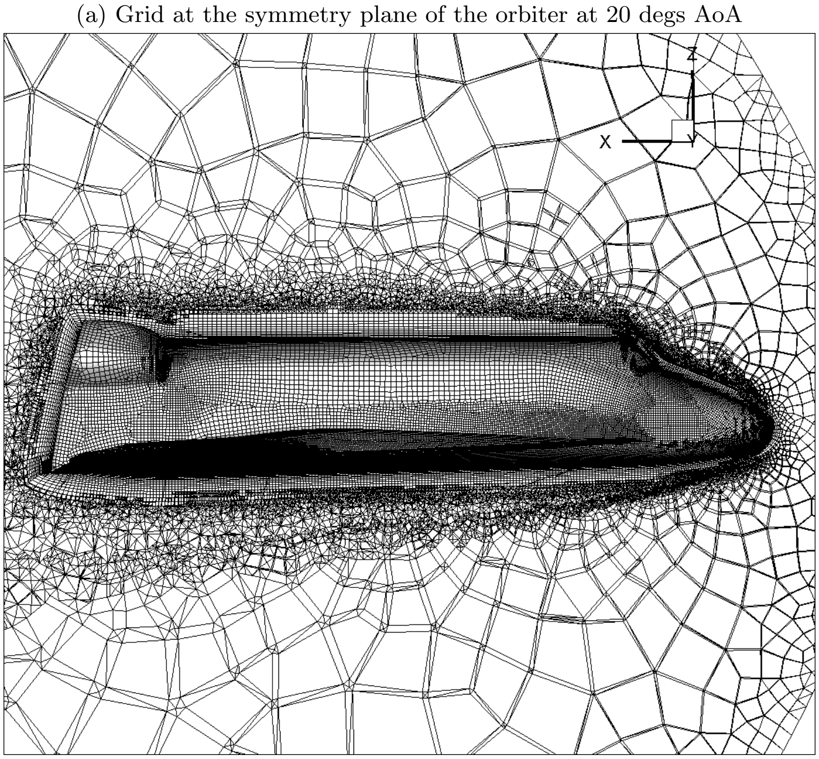

(b) Adapted grid at the symmetry plane of the orbiter at 20 degs AoA

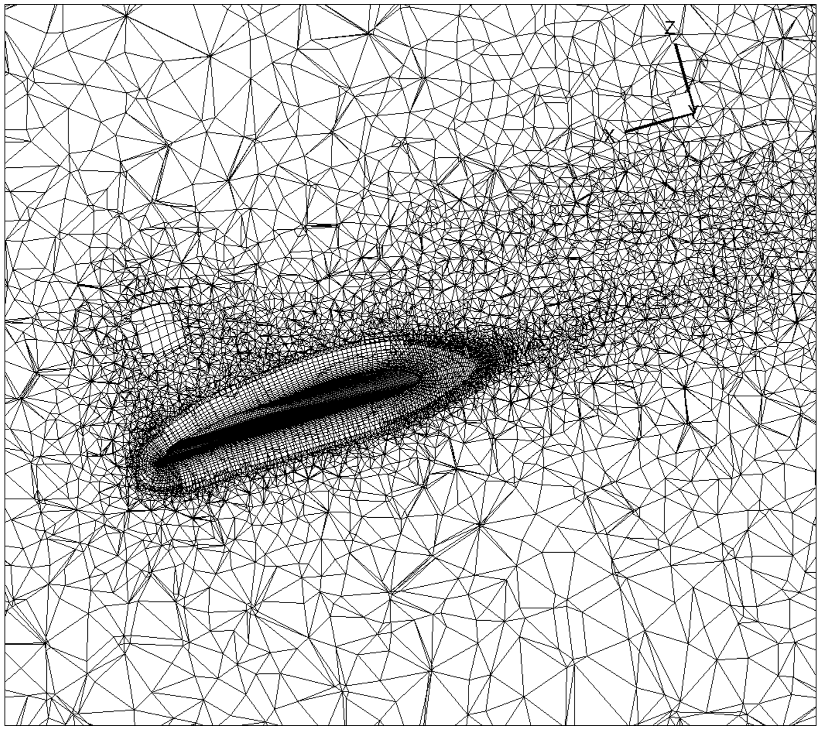

(a) Grid at the midspan of the wing of the orbiter at 20 degs AoA

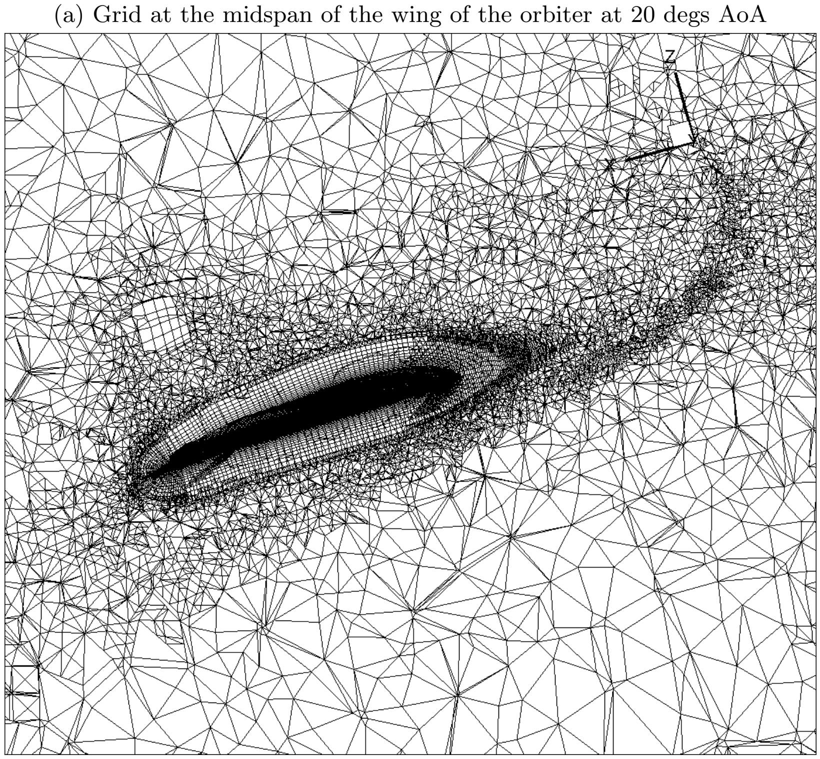

(b) Adapted grid at the midspan of the wing of the orbiter at 20 degs AoA

3.5.3 Table of force coefficients

Case [°]	C_L [-]	C_D [-]
20	0.341	0.174
Adapted 20	0.342	0.173

3.5.4 Fluent settings used to adapt grid

I forgot to keep track of what my exact settings were. However, I went back and recreated the settings based on what I remember. Admittedly, the 50% increase in number of cells was much larger than 10% expected. Nevertheless, even with this large increase, the differences are subtle. The most distinct difference in the mesh around the fuselage is on the "belly" of the Orbiter, while increased mesh density can be somewhat observed at the nose and turning corners of the Orbiter. The wing saw an denser mesh all around. The coefficients of lift and drag were not significantly altered. The settings of the gradient adaptations were approximately as follows,

- Options: Refine
- Method: Gradient
- Normalization: standard
- Gradients of: Pressure, static pressure
- Refine Threshold: 200
- Max: 11,190
- Min: 2.588e-05

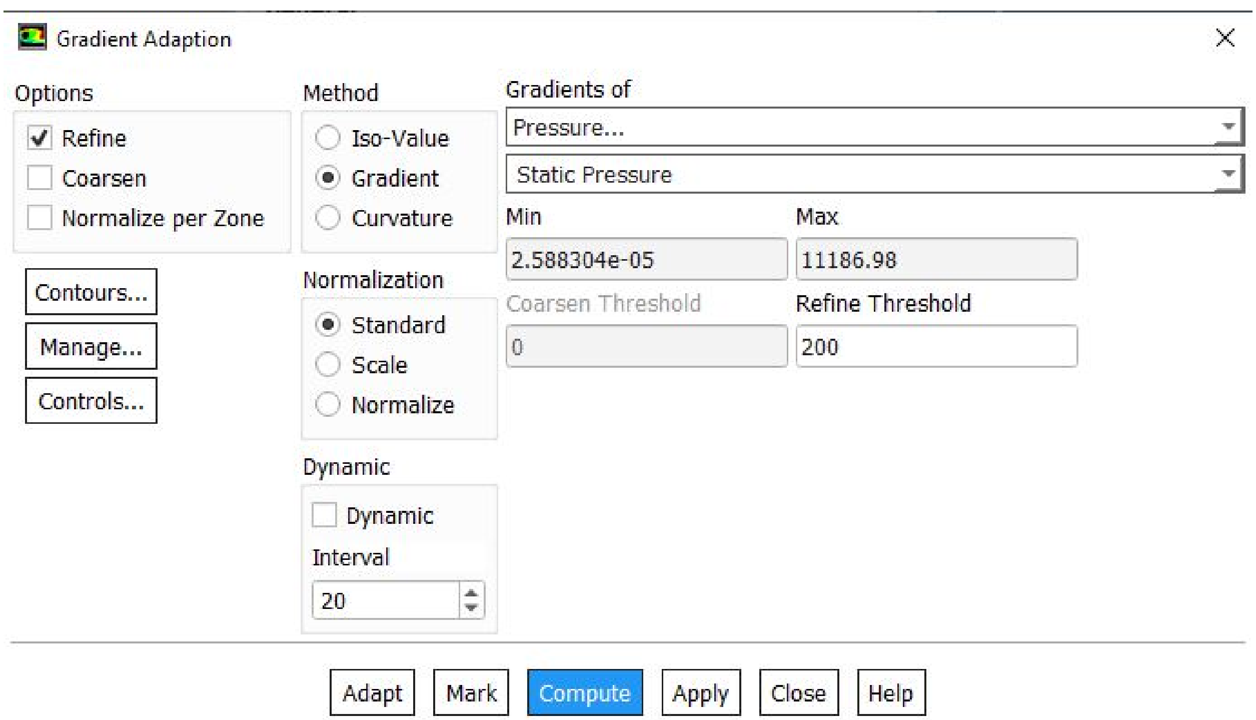

Figure 21: Grid adaptation settings

The results of the adaptation are summarized in the screenshot below,

```
>> 4 Stored Partitions:
   -----------------------------------------------------------------------
   Collective Partition Statistics:        Minimum   Maximum   Total
   -----------------------------------------------------------------------
   Cell count                              533069    575426    2203608
   Mean cell count deviation               -3.2%     4.5%
   Partition boundary cell count           5258      10268     32967
   Partition boundary cell count ratio     0.9%      1.9%      1.5%

   Face count                              1406814   1443780   5688939
   Mean face count deviation               -1.4%     1.2%
   Partition boundary face count           6621      12897     20465
   Partition boundary face count ratio     0.5%      0.9%      0.4%

   Cell weights                            3e+06     4e+06     1e+07
   Mean cell weight deviation              -20.7%    7.3%

   Partition neighbor count                2         3
   -----------------------------------------------------------------------
   Partition Method                        Metis
   Stored Partition Count                  4
Done.

   Smoothing partition boundaries...
 Dump usage: 1375480 cells, 3375228 faces, 701471 nodes

 Dump usage: 2203608 cells, 5688939 faces, 1355967 nodes

 Grid size ( original /   adapted /    change)
     cells (  1375480 /   2203608 /    828128)
     faces (  3375228 /   5688939 /   2313711)
     nodes (   701471 /   1355967 /    654496)
```

Figure 22: Grid adaptation summary

Appendix

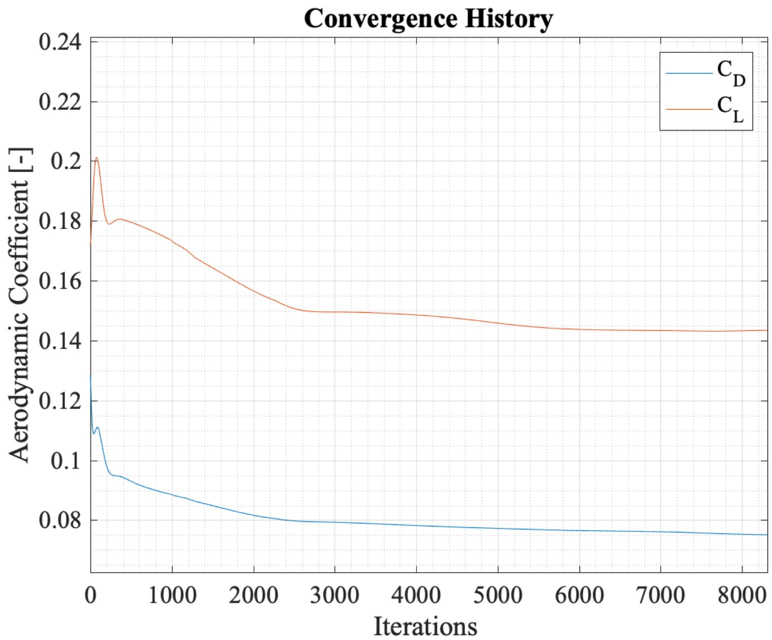

Figure 23: Convergence history for AoA = 10°

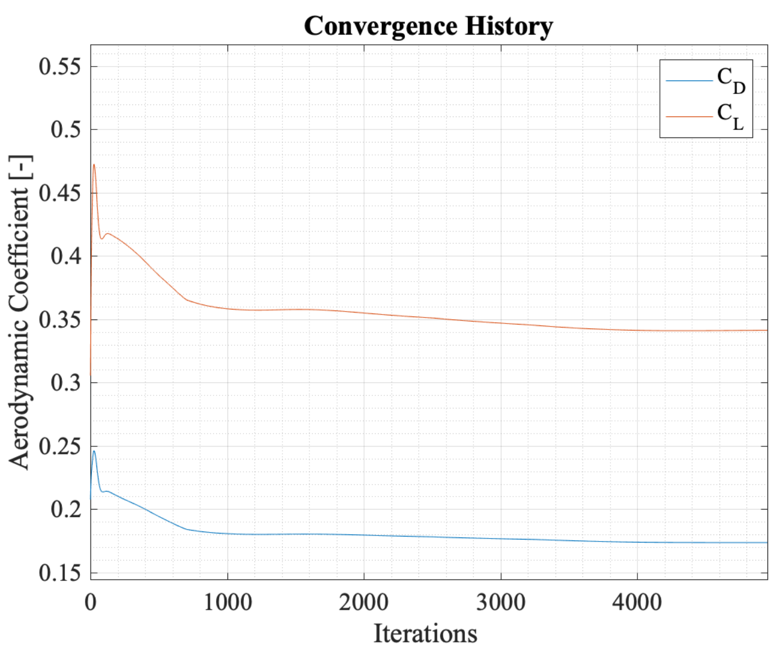

Figure 24: Convergence history for AoA = 20°

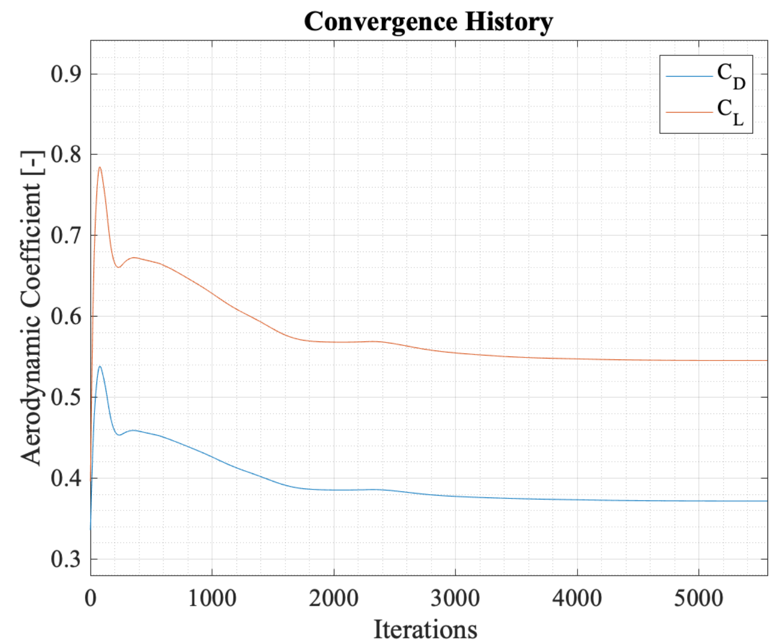

Figure 25: Convergence history for AoA = 30°

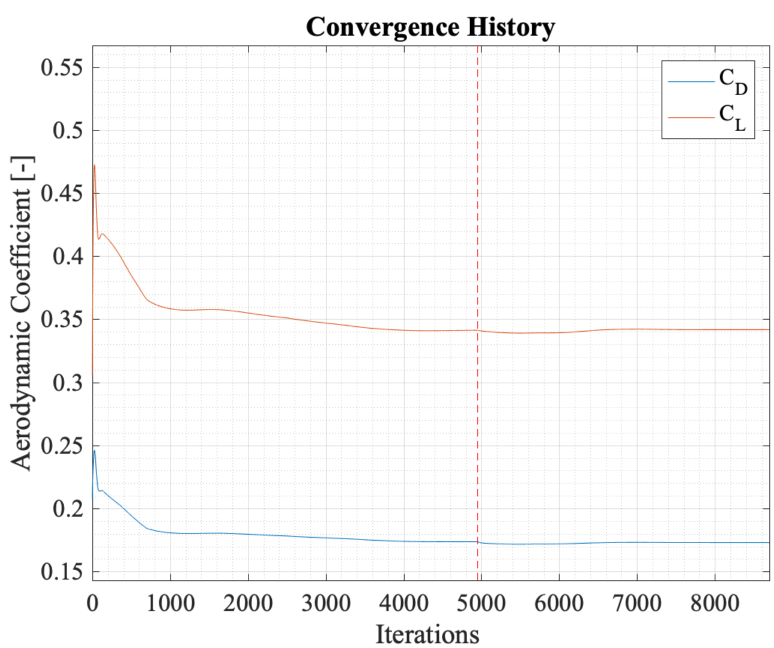

Figure 26: Convergence history with adaption for AoA = 20°; red dashed-line indicates where iterations for the refined mesh began.

References

[1] John D. Anderson. *Modern Compressible Flow with Historical Perspective*. McGraw Hill Education, 2003.

[2] Rui Dilão and João Fonseca. Dynamic guidance of gliders in planetary atmospheres. *American Society of Civil Engineers*, 1(29), 1 2016.